

LONGSHORE SEDIMENT TRANSPORT RATE MEASURED BY SHORT-TERM IMPOUNDMENT

By Ping Wang¹ and Nicholas C. Kraus,² Member, ASCE

ABSTRACT: The total longshore sediment transport rate in the surf zone was measured at a temporary groin installed at Indian Rocks Beach, west central Florida. Approximate mass balance between updrift accumulation and downdrift erosion, which served as an indicator of reliability, was obtained in four of the six runs, which were subjected to further analysis. Magnitudes of three of the four transport rates were considerably lower than predictions by the Coastal Engineering Research Center formula calculated based on contemporaneous measurements of the breaking waves. Error analysis indicated that the determination of the longshore wave-energy flux factor carried a 22–48% maximum uncertainty, and the measured volume-change rate carried a 22–43% uncertainty. The combined uncertainties produce a 40–90% maximum uncertainty in determination of the empirical transport coefficient K appearing in the Coastal Engineering Research Center formula. Comparable or greater uncertainty in K -values probably exists in the total database available for calibrating predictive formulas. The range in values of K in these measurements cannot be explained by measurement error or uncertainty. Therefore, it is concluded that K is not a constant and that other factors may enter, such as breaker type, turbulence intensity, and threshold for sediment transport.

INTRODUCTION

Accuracy of predictive formulas for the longshore sediment transport rate in the surf zone depends on a limited number of field measurements that exhibit considerable scatter (Schoonees and Theron 1993; Komar 1998). High-quality measurements are needed to improve the accuracy of predictive empirical formulas and to understand their ranges of applicability. Most field measurements of the total rate of longshore transport have been made by three methods—sand tracer, impoundment, and streamer sediment traps. Other measurement methods have been used occasionally as, for example, morphology change (Moore and Cole 1960), suspended sediment pumping (Fairchild 1977), instantaneous suspended sediment sampling (Kana and Ward 1980), and trench infilling (Mangor et al. 1984). Transport rates measured at the same time scale tend to be consistent with each other but not with rates measured under different time scales.

Sand tracer measurements yield an average rate taken over 2–4 h through quantification of vertical (mixing depth) and horizontal (center of mass) distributions of tracers [e.g., Komar and Inman (1970) and Kraus et al. (1982)]. Streamer traps measure the transport rate by quantifying the sediment flux through the water column and across the surf zone over measurement intervals of 5–10 min (Kraus 1987; Rosati and Kraus 1989; Wang 1995, 1998). The impoundment method measures the longshore transport rate by quantifying morphological change by either blocking sand movement with a shore-normal structure or reducing the transport with a shore-parallel structure (Berek and Dean 1982; Bodge 1987; Bodge and Dean 1987; Dean 1989). Long-term impoundment studies (Berek and Dean 1982; Dean 1989) involve measurement of material blocked by permanent coastal structures, and the transport rates obtained typically represent averages over months. Watts (1953) correlated transport rates with the amount of sediment hydraulically bypassed at an inlet. He found that the daily average longshore transport rate could be

significantly larger than the rate obtained as a monthly average.

In short-term impoundment (Bodge 1987; Bodge and Dean 1987) as discussed here, the transport-blocking structure is temporary, and the structure is installed solely for measuring the longshore sediment transport rate. Transport rates obtained through short-term impoundment are averages taken over hours.

Technical difficulties of the three main measurement methods include quantification of tracer distributions, trap efficiency, quantification of 3D morphological changes in impoundment, hydrodynamic disturbance of measuring devices, and distinguishing longshore-transport signals from those produced by other processes. For longer-term measurements, changes induced by cross-shore transport from waves and tide must be identified and filtered to obtain the longshore transport rate. The three measurement methods have been compared by Bodge and Kraus (1991) and Wang et al. (1998a), who explored measurement inconsistencies. In particular, Bodge and Kraus (1991) noted apparent problems with the time interval for wave averaging in application of the Coastal Engineering Research Center (CERC) formula (Shore 1984) and, therefore, in the time interval over which the transport is measured.

Most of the reliable field data forming the basis of empirical longshore transport prediction formulas were obtained with sand tracers (Schoonees and Theron 1993). Long-term impoundment measurements [e.g., Bruno and Gable (1976), Bruno et al. (1980), Dean et al. (1982), and Dean (1989)] tend to confirm the order of magnitude of the transport rate found with tracers. Compared with results obtained with sand tracers, most measurements made by short-term impoundment and the streamer sediment trap have given transport rates one-tenth to one-fourth those found in long-term impoundment and with tracers.

Prior to the present study, to our knowledge, the short-term impoundment method had been applied only once in the field (Bodge 1987; Bodge and Dean 1987), probably due to its labor-intensiveness. A significant advantage of the impoundment measurement is that there is an internal check available through comparison of volumes of updrift accumulation and downdrift erosion. The volumes should be equal if the groin successfully functions as a total longshore transport barrier and the survey quantifies the entire area of seabed change. This quality check is valuable because of the uncontrollable nature of the field conditions. Such a direct reliability indicator does not exist for the other field-measurement methods. The impoundment technique can be expanded systematically in mea-

¹Asst. Prof. of Res., Coast. Studies Inst., Louisiana State Univ., 332 Howe/Russell Geosci. Complex, Baton Rouge, LA 70803.

²Res. Phys. Sci., U.S. Army Engr. Wtrwy. Experiment Station, Coast. and Hydr. Lab., 3909 Halls Ferry Rd., Vicksburg, MS 39180.

Note. Discussion open until November 1, 1999. To extend the closing date one month, a written request must be filed with the ASCE Manager of Journals. The manuscript for this paper was submitted for review and possible publication on May 14, 1998. This paper is part of the *Journal of Waterway, Port, Coastal, and Ocean Engineering*, Vol. 125, No. 3, May/June, 1999. ©ASCE, ISSN 0733-950X/99/0003-0118-0126/\$8.00 + \$.50 per page. Paper No. 18383.

surement duration and size of the structure, holding the possibility of bridging the gap between short- and long-term measurements to resolve the issue of sampling interval and suitable wave averaging.

In the present study, the total longshore sediment transport rate in the surf zone was measured by short-term impoundment under low-wave energy conditions (breaker heights < 0.5 m). The objectives were to develop and refine the promising and yet relatively unused short-term impoundment procedure and to measure the total longshore sediment transport rate. Mass balance at the updrift and downdrift sides of the temporary groin was examined, as well as response of the beach profile and shoreline to the installation of the groin. An error analysis was conducted to quantify uncertainties associated with the measurement of change in beach volume and calculation of transport rate by the CERC formula.

STUDY AREA AND METHODOLOGY

The measurements were conducted on Indian Rocks Beach, located in west central Florida. The tidal range at the study site is relatively small, typically within 0.8 m, a favorable condition because tidal range has significant influence on determining the effective length of a groin. Five of the six runs were conducted during daily tidal ranges of <0.4 m, and the other run was conducted in a range of ~0.6 m. The surf zone is composed of shelly sand, with a mean grain size of ~0.35 mm (Wang et al. 1998b). The experiments were conducted on a straight stretch of beach distant from the influence of inlets and any artificial or natural structures. Many of the nearshore beach profiles were characterized by a steep step, referred to as a plunge step, at the breaker line. Waves broke predominantly by collapsing at the plunge step during the data collection. Surf-zone width during the study period was relatively narrow, ranging from approximately 3 to 9 m.

A low-cost and efficient short-term impoundment procedure was developed for data collection under low-wave energy conditions along microtidal coasts, such as at Indian Rocks Beach. This design is suitable for many Gulf of Mexico beaches, estuarine shorelines in microtidal settings, and lake shorelines.

Impoundment Design

An optimal short-term impoundment procedure should not allow sediment bypassing, minimize hydraulic disturbance, and be efficiently installed and removed. For low-wave energy, microtidal conditions, a temporary groin can be constructed of wood sheeting (2–3 cm thick) (Fig. 1). The groin was composed of several sections as determined by the width of the surf zone. A section length of ~3 m was found convenient for transportation and installation. The length of the groin can be adjusted in the field by adding or removing sections. An ~10-cm overlap between adjacent sections was found necessary to prevent leaking through the section joints. Sections were held together with clamps. The length of the groin should be adjustable to accommodate changes in water level to maintain extension well beyond the surf zone. The board was installed by pounding the angle irons (Fig. 1) into the sand. The angle irons also served as anchors for the groin. Boards with different heights were set according to the local depth in the surf zone and extended well above the crest of the waves to prevent overpassing. Installation of five 3-m sections was completed within 30 min by three people.

Experience showed that sandbag liners (10–15 cm in diameter) (Fig. 1) were needed along the base of the board to prevent bottom scour induced by the swash and wave breaking. The sandbags, filled at the site, successfully prevented scour during the measurement, which can lead to leakage of sand under the board and weakening of its foundation.

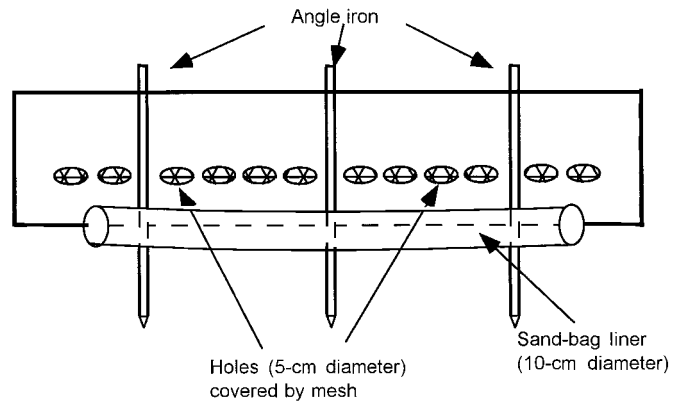


FIG. 1. Schematic Design of Impoundment Board (Temporary Groin) and Sandbag Liner

After the first two runs, holes were drilled through the impoundment board (Fig. 1) to reduce disturbance of the longshore current by the structure and the pressure exerted on it by the current. The holes were covered with 63- μ m sieve cloth to allow passage of water but not sediment. The size and number of the holes (of 5-cm diameter and one row in the present study) should be determined based on specific field conditions. The holes appear to be most effectively located at approximate mid-water-depth position. Observation indicated that the holes reduced development of a rip current on the updrift side of the groin. Rip-current development, also observed by Bodge (1987) in laboratory and field impoundment studies, was identified as an undesirable hydraulic disturbance of a groin-type impoundment structure. Water flowing through the holes acts to maintain the longshore current directly on the downdrift side of the groin, which tends to transport sediment alongshore and out of the shadow or wave-shelter zone of the groin.

The temporary groin constructed by Bodge (1987) consisted of a stack of three large sand tubes because of the relatively high waves encountered. The groin had a low profile to reduce its hydraulic disturbance yet minimize sediment overpassing. Bodge (1987) concluded that an optimal groin was one with crest located (1) just at or slightly below the upper envelope of the swash and waves across the foreshore and inner surf zone; (2) just at or below the mean-water level across the midsurf zone; and (3) at about half the local wave height above the bed across the outer surf zone. This prescription may be appropriate for actual field groins, but for impoundment measurements, high groins with holes covered by sieve cloth assure no loss of sediment by overtopping and promote continuity of the longshore current (minimum rip current) at the structure.

Field Procedure

The procedure consisted of establishing a survey grid, a preinstallation beach profile survey, groin installation, and as many as three postinstallation beach surveys. A schematic layout is depicted in Fig. 2. The actual layout was determined based on specific beach and wave conditions. The procedure was developed so that a run from preinstallation survey to groin removal could be completed during daylight.

Survey grid-line spacing was identical updrift and downdrift of the groin. The symmetrical grid provided a uniform reference for comparison of updrift accumulation and downdrift erosion. Intervals between adjacent survey lines increased with distance from the groin, expanding from 0.5 to 4 m. The telescoping grid captured the rapid changes that occurred in the vicinity of the groin but allowed sufficient updrift and downdrift areas to be surveyed to encompass all morphologic change. Two control lines were also surveyed, one each located far updrift and downdrift, outside the anticipated area of

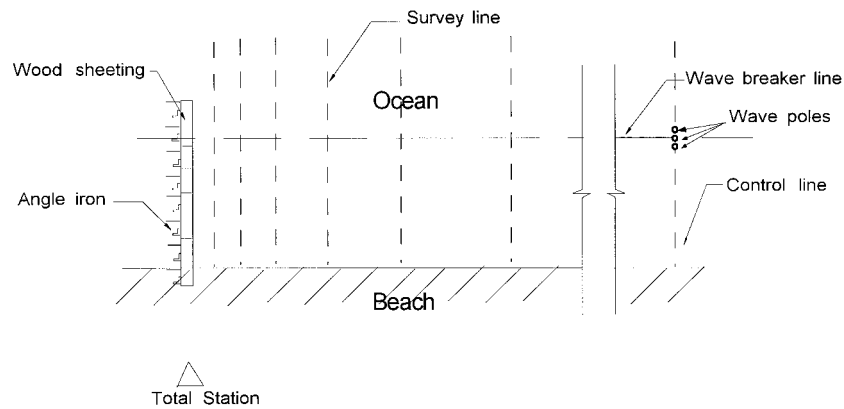


FIG. 2. Schematic Layout of Field Operation; Only Half of Mirror-Image Layout Is Illustrated

TABLE 1. Typical Time Requirements for Impoundment Procedure

Operation (1)	Approximate elapsed time (h) (2)
Grid setup	1
Preinstallation survey	1–1.5
Groin installation	0.3–0.5
Time interval between installation and postsurvey	1–2
Postinstallation surveys	1–1.5
Groin removal	0.2–0.5

groin influence (initially assumed to be located beyond at least three groin lengths) over the total run interval. As discussed in the following sections, during a measurement interval of <5 h, the area of influence was located within two groin lengths. The control lines were established to monitor possible changes in beach volume and shoreline position caused by processes other than longshore transport. Such changes are expected from tidal water-level fluctuations and from cross-shore sediment transport by waves.

It was assumed that the longshore sediment transport was uniform along the straight study beach, and the beach did not undergo significant local morphological change under the approximately constant incident waves. Therefore, morphological change measured beyond the influence of the groin is attributed to processes other than longshore transport and should be subtracted from changes measured within the impoundment area. Morphological change caused by tidal water-level fluctuations (e.g., the cross-shore movement of the plunge step) was observed.

A uniform pace, starting at one control line and finishing at the other, was followed during all pre- and postinstallation surveys. A uniform pace was convenient for the data reduction, discussed in the following section. The beach was surveyed with a SOKKIA SET4B electronic total station. The survey rod was shortened to 1.5 m to minimize errors that could be introduced by slight tilting of the rod during operation. The beach-profile surveys started landward at a baseline located above the uprush limit and extended at least one surf-zone width seaward of the surf zone. Times for operations with a three-person crew in a typical measurement run are summarized in Table 1.

The incident wave breaker height and period were measured by video taping waves incident on scaled poles placed at the breaker line at the site (Ebersole and Hughes 1987). Two to three poles with 2-cm scales were placed perpendicular to the shoreline (Fig. 2) at the breaker line (a narrow zone where waves broke). Wave height was measured at the pole closest to the breaking wave. Fifteen to 20 breaker heights and wave periods were digitized from the continuous video recording at

~30-min intervals. Five to 10 incident breaker angles were measured with a handheld compass by each of the three crew members to minimize reader bias. Approximate shoreline position was also identified by the rod holder during the beach survey.

Data Reduction

Survey data reduction and calculation of the transport rate consisted of (1) calculating profile-volume change between pre- and postinstallation surveys; (2) removing volume change not related to longshore transport impoundment as estimated from the control lines; (3) calculating total updrift and downdrift volumes; and (4) calculating the total rate of longshore sediment transport. The transport rate was obtained by dividing the volume change by the respective average times between groin installation and updrift and downdrift surveys.

Profile-volume change (in units of cubic meters per meter) was calculated from the pre- and postinstallation surveys. Volume change caused by processes other than longshore sediment transport $v_{\text{non-LST}}$ was estimated by the average of the profile volume change measured at the control lines as

$$v_{\text{non-LST}} = \frac{1}{2} (v_{c-u} + v_{c-d}) \quad (1)$$

where v_{c-u} and v_{c-d} = volume change measured at the updrift and downdrift control lines, respectively. A rate of profile-volume change not related to longshore transport $R_{\text{non-LST}}$, and attributed mostly to tidal water level change in the present study, is calculated as

$$R_{\text{non-LST}} = \frac{v_{\text{non-LST}}}{\Delta t_c} \quad (2)$$

where Δt_c = elapsed time between two surveys on the same control line. Profile-volume change at a particular survey line i $v_{\text{LST-}i}$ associated with longshore transport can then be calculated as

$$v_{\text{LST-}i} = v_i - R_{\text{non-LST}} \times \Delta t_{pi} \quad (3)$$

where v_i = volume change measured at profile i ; and Δt_{pi} = time interval between completion of groin installation and completion of the survey of profile i , assuming a constant $R_{\text{non-LST}}$ during the measurement period.

Given the short distance between survey lines and gentle change in the shoreline curvature, the volume change between adjacent lines can be represented by the volume of a right trapezoidal prism. The total volume change (in units of cubic meters) induced by longshore transport at the updrift side $V_{u\text{-total}}$ was then calculated as

$$V_{u\text{-total}} = \sum_{i=1}^m \left(\frac{\Delta x_p}{2} (v_{\text{LST-}i} + v_{\text{LST-}(i+1)}) \right) \quad (4)$$

where Δx_p = distance between two adjacent survey lines; and m = number of updrift survey lines excluding the control line. The total volume change induced by longshore transport at the downdrift side $V_{d-total}$ was similarly calculated as

$$V_{d-total} = \sum_{i=1}^n \left(\frac{\Delta x_p}{2} (v_{LST-i} + v_{LST-i+1}) \right) \quad (5)$$

where n = number of downdrift survey lines excluding the control line. For the present survey grid layout, $m = n$.

The total longshore transport rate was calculated from updrift accumulation Q_u as

$$Q_u = \frac{V_{u-total}}{\Delta t_u} \quad (6)$$

and from downdrift erosion Q_d as

$$Q_d = \frac{V_{d-total}}{\Delta t_d} \quad (7)$$

where Δt_u = elapsed time from the groin installation to the midpoint of the updrift survey grid and similarly for Δt_d . The above calculations were based on the assumption of a steady rate of longshore transport over a typical 1- to 3-h interval.

The time interval between groin installation and the beginning of the postinstallation survey was typically 1.5–2 h. The postinstallation survey typically took ~1 h. The measured volumes of updrift accumulation $V_{u-total}$ and downdrift erosion $V_{d-total}$ were not the same because the time intervals between groin installation and the surveys on the updrift and downdrift grids were different, caused by the time needed for the survey using one total station. However, the transport rates calculated from (6) and (7) should be comparable if the assumption of constant longshore transport rate and $R_{non-LST}$ holds. During a short measurement period under constant waves, the assumptions of constant longshore transport rate and constant $R_{non-LST}$ are justified.

RESULTS

Run 1, the first of the six runs, was conducted during normally incident waves. Although the longshore transport rate was negligible, the field procedure was tested and refined. The design of the groin, as well as the survey-grid layout, was modified significantly after Run 2. The improvements included (1) adding four more survey lines to the previous seven lines updrift and downdrift; (2) increasing survey line density near the groin; (3) extending the survey grid to about two groin lengths instead of 1.5 lengths; (4) moving the control line to approximately four groin lengths instead of three lengths; (5) adding mesh-covered holes in the board to reduce rip-current development; and (6) adding sandbag liners to prevent scour along the board. These modifications were implemented to

reduce the groin's hydraulic disturbance, to allow minimal bypass and/or leakage, and to ensure complete coverage of the survey grid.

Field Conditions and Groin Performance

Constancy of the waves is of central concern to data collection designed under the assumption of a constant longshore transport rate during a measurement period of hours. The six runs were conducted under mild summer wave conditions occurring from April to September. The daily afternoon breeze generated by land-water temperature differences modified the incident waves during two of the runs. Reversal of incident wave direction (i.e., reversal between updrift and downdrift sides) occurred during Runs 3 and 5.

The sandbag liners along the board performed satisfactorily inside the surf zone and usually became buried, especially in the swash zone, as the impoundment continued. However, at and directly seaward of the breaker line, scour along the board persisted, and a scour hole often developed toward the end of the runs, typically 5 h or more after groin installation. Additional sandbags were installed to mitigate the scour but were effective only for a short time.

At longer elapsed time, it was possible that the influence of the groin moved beyond the survey grid, especially at the downdrift side. Therefore, volume changes measured between the Pre- (initial) and Post 1 (the first time interval) surveys are more reliable, because of the time factor (constant wave conditions) and impoundment performance, as compared to later surveys (Post 2 or Post 3). Based on lack of constancy of wave conditions and reduced performance of the groin caused by scour at the breaker line, several measurements were discarded. Four measurements (Table 2) satisfying the aforementioned acceptance criteria (constant waves, volume change contained within the survey grid, minimal influence of the rip current, and negligible sand underpassing at the board) were subjected to analysis, as discussed in the following.

Patterns of Accumulation and Erosion

Significant sediment accumulation occurred at the updrift side of the groin [Fig. 3(a)] with corresponding erosion at the downdrift side [Fig. 3(B)]. As much as a 30-cm elevation change occurred between the lower swash zone and the breaker line during an impounding interval of 120 min during Run 5, in both the accreted and the eroded areas. Most of the accumulation and erosion took place in the surf zone. The accumulation patterns also support the finding that under collapsing breakers, the contribution in the swash zone can be significant (Bodge 1986; Bodge and Dean 1987). It is noted that for the studied beach under low-wave energy and collapsing breakers, the swash zone compromised a significant portion of the surf zone.

TABLE 2. Summary of Reliable Measurement Runs

Run number (1)	Breaker Height		Breaker Angle		Wave Period		Beach slope ^c (8)	Surf similarity parameter (9)	Q_u/Q_d (10)
	RMS (cm) (2)	SD ^a (cm) (3)	Mean (degrees) (4)	SD ^b (degrees) (5)	Mean (s) (6)	SD ^b (s) (7)			
2: Pre-Post 1	14.0	3.8	8.2	2.7	3.8	0.8	0.12	1.52	0.61
4: Pre-Post 1	20.3	5.2	13.4	2.5	3.6	0.8	0.09	0.90	1.06
5: Post 1-Post 2 ^d	28.5	7.2	19.7	6.3	3.0	0.6	0.13	0.91	1.65
6: Pre-Post 1	38.3	7.8	4.9	4.5	4.3	1.2	0.12	1.04	1.15

^aThe means and SD of breaker height and wave period were determined based on 60 measurements. The SDs for Run 2 were calculated based on 15 measurements.

^bThe mean and SD of incident breaker angle were determined based on 20 measurements.

^cAverage of beach slope (from shoreline to breaker line) at two control lines.

^dPost 1 survey was started shortly after strong afternoon breeze, which changed wave conditions. Wave conditions remained constant between Post 1 and Post 2, although the condition was different from that between Pre- and Post 1.

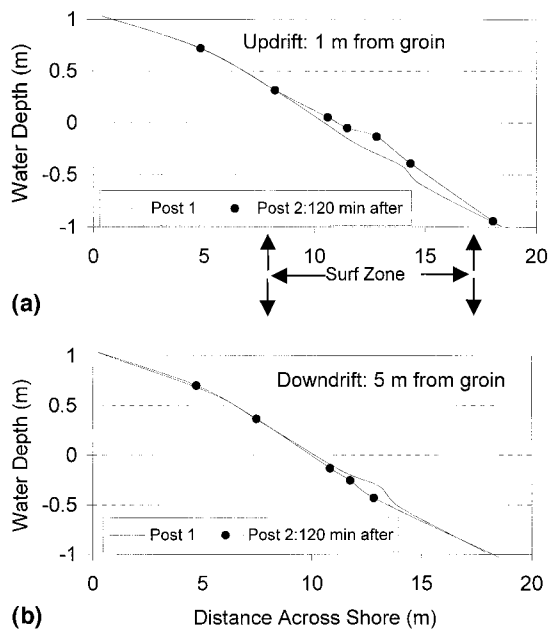


FIG. 3. Examples of Updrift Accumulation and Downdrift Erosion from Run 5

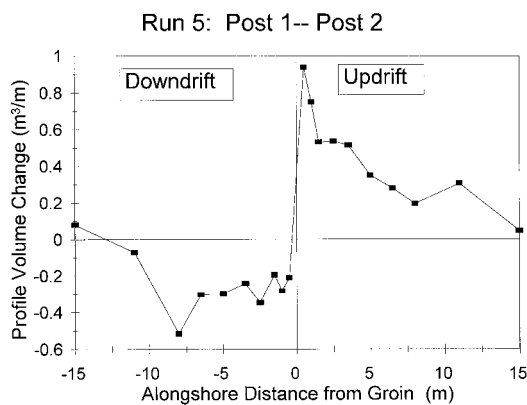


FIG. 4. Alongshore Distribution of Profile-Volume Change

The planforms of updrift accumulation and downdrift erosion alongshore differed. Maximum accumulation typically appeared directly updrift of the groin (Fig. 4), as expected. The broad maximum in downdrift erosion was typically located 3–7 m from the groin, or 35–80% of the groin length during the period of the experiment. The downdrift-displaced erosion pattern was caused by wave sheltering by the groin and was probably influenced by the longshore current that passed through the holes in the groin.

The shoreline advanced on the updrift side of the groin and receded on the downdrift side, as expected. The maximum shoreline advance was located a short distance from, but not directly updrift of, the groin (Fig. 5). A seaward flow along the impoundment board at the updrift side, which was responsible for the scour at the groin, was observed during the measurements. The flow carried some of the sand seaward and out of the surf zone, resulting in less shoreline advance at the groin than that at a short distance updrift. The amount of offshore sediment transport along the groin is expected to depend on structure permeability and the strength of the rip current adjacent to the groin. The influence of offshore transport was more apparent for Run 2 with the impermeable groin (before the mesh-covered holes were implemented) than for Runs 4 and 5, for which holes in the board allowed controlled passage of water (Fig. 5).

Maximum downdrift shoreline recession occurred a short distance from the groin, similar to the pattern in volume

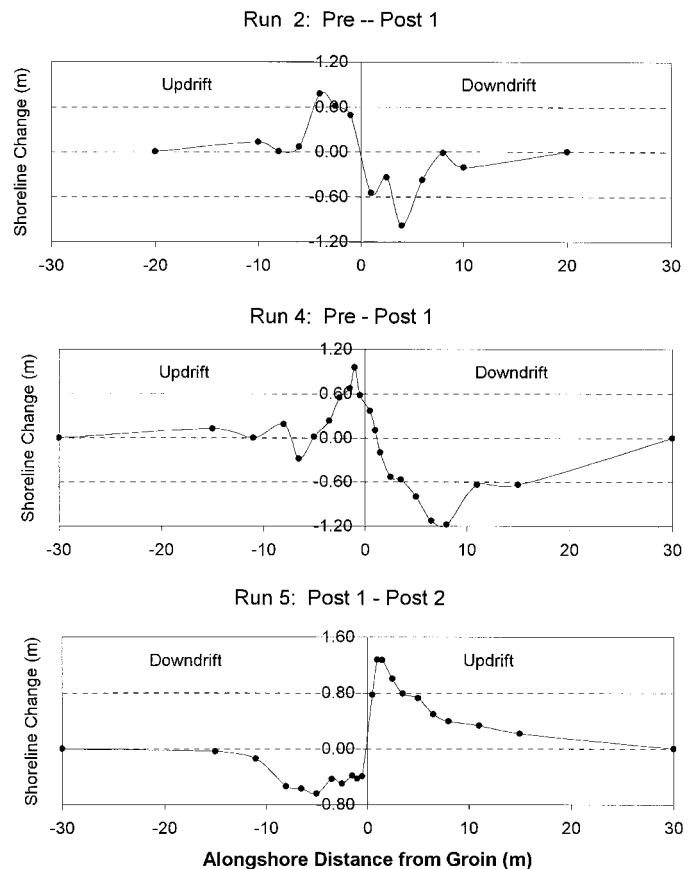


FIG. 5. Shoreline Change Patterns in Vicinity of Groin

change. Wave sheltering of the groin tended to protect the shoreline directly downdrift. Accumulation and erosion patterns may be different updrift and downdrift of the groin, as noted by Bodge (1987), owing to the differences in longshore current gradients alongshore and in wave conditions (reflection updrift, diffraction downdrift). However, the total volume should be conserved if the temporary groin functions as a total longshore transport barrier.

Total Rate of Longshore Sediment Transport

A significant advantage of the impoundment method over other field-measurement methods is that change in beach volume can be measured simultaneously both updrift and downdrift of the structure. Because volume should be conserved, the updrift and downdrift measurements provide an indicator of reliability, defined here as the ratio of Q_u and Q_d . The rate of volume change, instead of volume itself, was used to compensate the time needed for the survey. The reliability indicator provides an objective parameter for evaluating the performance of the groin as a total trap and quality of the entire measurement procedure under noncontrollable field conditions.

The CERC formula (Shore 1984) is the most commonly applied predictive formula for the total longshore sand transport rate Q_c in the surf zone, and it has often been used as a benchmark for other empirical formulas. The CERC formula takes the longshore sediment transport rate as proportional to the longshore wave-energy flux factor

$$Q_c = KAP_t \quad (8)$$

in which K is the transport coefficient to be empirically determined, and

$$A = \frac{1}{(\rho_s - \rho)g(1 - p)} \quad (9)$$

is a conversion factor containing properties of the sediment with ρ_s = sediment density; ρ = water density; g = gravitational acceleration; p = porosity of sediment; and P_l = longshore wave-energy flux factor (Komar 1998) at depth-limited wave breaking, given by

$$P_l = \frac{1}{16\sqrt{\gamma}} \rho g^{3/2} H_{brms}^{5/2} \sin(2\theta_b) \quad (10)$$

where γ = wave breaker index (ratio of wave height to water depth at breaking); H_{brms} = root-mean-square breaking wave height; and θ_b = breaking wave angle. For a given beach, the CERC formula requires input of only the breaker height and angle. The porosity of the shelly sand in the study area was measured and found to be ~ 0.4 .

The CERC formula was originally developed by observation of hydraulically bypassed quantities at an inlet on the Atlantic Ocean coast of the United States (Watts 1953) and by monitoring of dredged material placed on a Pacific Ocean coast beach (Caldwell 1956). The formula has been validated, and its confidence improved through sand tracer measurements (Komar and Inman 1970) and subsequently verified with long-duration impoundment measurements [summarized by Dean (1989) and Komar (1998)].

For root-mean-square (RMS) wave height, a value of 0.77 was originally determined by Komar and Inman (1970) and is recommended in the *Shore Protection Manual* (Shore 1984). In a recent summary, Komar (1998) arrived at a slightly lower K -value of 0.70, and Schoonees and Theron (1994) analyzed the 46 most reliable of 240 measurements compiled to determine a K -value of 0.41. Based on 29 streamer-trap measurements for a low-wave energy setting ($H_{brms} = 0.1\text{--}0.8$ m), Wang et al. (1998a) found a best-fit value of 0.08. Such low values were also obtained by Kraus and Dean (1987) and Kraus et al. (1988) with streamer traps for moderate waves ($H_{brms} = 0.5\text{--}1.1$ m) similar to those occurring in past tracer measurements.

Existing data as summarized above suggest that the empirical K may not be a constant. A possible relationship between K and the surf-similarity parameter (controlling breaker type) has been discussed in several studies [e.g., Kamphuis and Readshaw (1978), Vitale (1981), Ozhan (1982), Bodge (1987), and Bodge and Kraus (1991)]. The surf-similarity parameter is defined as

$$\xi_b = \frac{\tan \beta}{\sqrt{H_{brms}/L_0}} \quad (11)$$

where $\tan \beta$ = beach slope, and L_0 = deepwater wavelength. Values of the surf-similarity parameter are given in Table 2. Run 2 had a significantly higher value of 1.5 resulting from a steep beach slope and small wave height, as compared to the other three runs (~ 1.0). However, values of the surf-similarity parameter in the present experiments cover a limited range and may have utility through inclusion with other data sets.

Three of the four accepted measurements (Table 2) were obtained within 3 h of groin installation (i.e., from Pre- to Post

1 measurements. Post 2 surveys were usually started ~ 4 h after groin installation and completed within 1 h. Bottom scour at the breaker line at the board had increased influence on Post 2 measurements as compared with Post 1. An exception was Run 5. During the Pre- to Post 1 interval, the waves were small and incident at a small angle, and little beach-volume change was measured. After groin installation, there was a rapid increase in wave height and incident angle. The Post 1 survey was expedited to 75 min after groin installation instead of 120 min as planned to minimize ambiguity associated with unsteady waves accompanying rapid development of a strong afternoon breeze. The waves remained nearly constant during the interval between the Post 1 and Post 2 surveys.

The ratios of the rates of updrift accumulation and downdrift erosion (defining the reliability indicator) of the four measurements ranged from 0.61 to 1.65 (Table 2), with an average of 1.12 and a standard deviation of 0.43 (38% of the mean). The empirical coefficient K (average of the updrift and downdrift values) ranged from 0.04 to 0.54 (Table 3), with an average of 0.20 and a standard deviation of 0.23 (118%). Significant scatter was found from the four measurements (Fig. 6). In this figure, the horizontal and vertical bars denote estimated uncertainties according to Table 3. A linear relationship between longshore transport rate and energy flux factor as contained in the CERC formula is not apparent in the present measurements that, however, cover a narrow range of transport magnitude.

Magnitudes of three of the four K values agreed with those obtained with streamer traps (Kraus et al. 1988; Wang et al. 1998a). The highest K value, 0.54, which fell in the range of values obtained with tracer and long-term impoundment, was obtained from Run 2 with the impermeable groin. It is noted that the rate from Run 2 carried the highest calculation error (discussed in the following section) of 48% because of the small wave height. Run 2 also differs from the other three runs in having a greater transport rate on the downdrift side and a much higher surf-similarity parameter than the other three (Table 2).

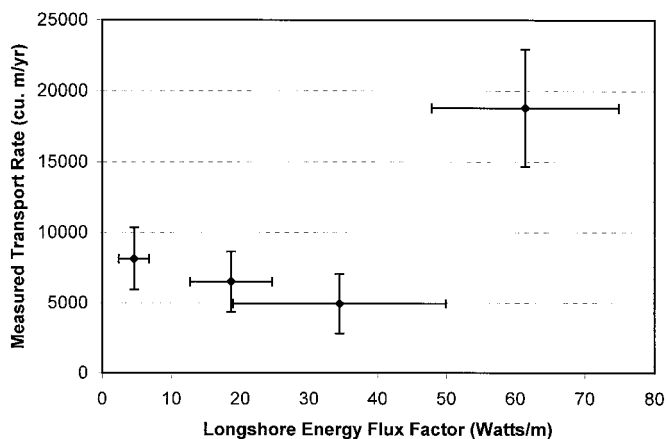


FIG. 6. Measured Longshore Transport Rates versus Longshore Energy Flux Factor

TABLE 3. Estimated Uncertainty in Determination of Longshore Sediment Transport Rate

Run number (1)	Measured Rate		Variation in energy-flux factor $\delta P_l/P_l$ (%) (4)	Best-fit variation in K (%) (5)
	Q_m ($Q_u:Q_d$) ($m^3/year$) (2)	$\delta Q_m/Q_m^a$ (%) (3)		
2: Pre-Post 1	8,132 (6,149:10,116)	27	48	0.541 ± 0.390 (75)
4: Pre-Post 1	6,505 (6,693:6,317)	33	32	0.107 ± 0.067 (65)
5: Post 1-Post 2 ^a	18,813 (23,412:14,214)	22	22	0.094 ± 0.041 (44)
6: Pre-Post 1	4,948 (5,291:4,604)	43	45	0.044 ± 0.037 (88)

^aMeasured rates and associated uncertainties are averages of updrift and downdrift values.

Error Analysis

An error analysis was performed to determine bounds for both the calculations of rate of volume change and the wave-energy flux factor. Table 4 lists instrument and operational uncertainties in the impoundment technique as conducted in this study. A small error associated with breaker-height measurement enters because some of the waves broke a short distance from, instead of exactly at, a wave pole. Error in breaker angle measurement is introduced in the visual alignment of the compass with the breaker line. Uncertainty in the topographic survey is caused by instrument limitations, possible slight tilt of the survey rod, and small deviations in reoccupation of the survey lines (Kraus and Heilman 1998).

Grid points on the two base lines were surveyed repeatedly, and the average of the differences of the 233 repeated surveys gave a standard deviation of 0.5 cm as an operational estimate of vertical error. During the conversion from volume to transport rate, a uniform pace of the profile survey was assumed for the actual approximate uniform pace. A survey of each profile line typically took 3–4 min. The estimated 5-min uncertainty (Table 4) accounts for a possible deviation from the uniform pace. As discussed in the following [(13)], the deviation from a uniform pace contributes considerably, approximately 10–20%, to the uncertainty in determination of volume change.

Measurement uncertainties transfer to the volume and transport rate calculations [(4)–(7)]. In the following, the notation ΔX will denote a temporal or spatial change in the quantity X , and the notation δX will denote an error or uncertainty in X . For legibility, the notation δX is taken to carry both signs (i.e., $\delta X = \pm|\delta X|$) unless a \pm symbol appears before it, in which case δX is taken to be positive. The errors δX are assumed to be small, such that either $\delta X/X \ll 1$ or $\delta X/\Delta X \ll 1$, depending on the quantity considered. Accounting for measurement error, (6) and (7) are reexpressed through a Taylor series as

$$Q_m + \delta Q_m = \frac{\Delta V \pm \delta V}{\Delta t \pm \delta t} = \frac{\Delta V \pm \delta V}{\Delta t} \left(1 \pm \frac{\delta t}{\Delta t} \right) \\ = \frac{\Delta V}{\Delta t} \pm \left(\frac{\delta V}{\Delta t} + \frac{\Delta V}{\Delta t} \frac{\delta t}{\Delta t} + \frac{\delta V \delta t}{\Delta t^2} \right) \quad (12)$$

where Q_m and δQ_m = measured transport rate and its uncertainty, respectively; ΔV and δV = measured volume change and its uncertainty, respectively; and Δt and δt = elapsed time between two surveys and its uncertainty, respectively. In (12), the term containing the product $\delta V \delta t$ is of second order and is dropped. The percentage ratio of the uncertainty is

$$\left(\frac{\delta Q_m}{Q_m} \right) \% \approx \frac{\frac{\delta V}{\Delta t} \pm \frac{\Delta V \delta t}{\Delta t^2}}{\frac{\Delta V}{\Delta t}} \times 100 = \pm \left(\frac{\delta V}{\Delta V} + \frac{\delta t}{\Delta t} \right) \times 100 \quad (13)$$

From (4) and (5), the uncertainties associated with volume calculation δV can be determined as

TABLE 4. Estimated Uncertainty in Impoundment Measurements

Quantity (1)	Instrument (2)	Operation (3)	Total (4)
Breaker height δH_b (cm)	1	2	3
Breaker angle $\delta \theta_b$ (degrees)	<1	2	3
Horizontal distance (cm)	<1	2	3
Elevation δz (cm)	<0.2	0.3	0.5
Distance between survey lines δx_p (cm)	<1	4	5
Time δt (min)	Negligible	5	5

$$\delta V = \pm \sum_{i=1}^M \left(\frac{v_i + v_{i+1}}{2} \times \delta x_{pi} \right) \pm \sum_{i=1}^M (\delta v \times \Delta x_{pi}) \quad (14)$$

where δx_{pi} = uncertainty associated with the survey line spacing Δx_{pi} , and M = total number of profiles used in the volume calculation. The uncertainty associated with the profile-volume calculation δv , can be determined as

$$\delta v = 2\delta z \times Y_s \quad (15)$$

where Y_s = cross-shore distance over which the volume-change calculation was conducted, which is on the order of the width of the surf zone; and δz = uncertainty in elevation measurement.

The survey grid extended well beyond the active zone of longshore and cross-shore morphology change. Calculation of total volume change and the associated error analysis were conducted in regions where significant morphological changes occurred. Minor beach-profile change, defined as smaller than δv , was excluded. Small changes in profile volume were usually measured alongshore at survey lines distant from the groin (e.g., Fig. 4, at 15 m).

Measurement uncertainties obtained from (12)–(15) are summarized in Table 3 and fall between 22 and 43%. Measurement errors were relatively small for runs with great volume change (e.g., Run 5). Large measurement uncertainty was associated with small volume change under variable incident wave angle (e.g., Run 6) (Tables 2 and 3).

The uncertainty δQ_c in the longshore transport rate calculated by the CERC formula [(8)] is given by

$$\frac{\delta Q_c}{Q_c} = \frac{\delta K}{K} + \frac{\delta A}{A} + \frac{\delta P_l}{P_l} \quad (16)$$

in which δK , δA , and δP_l = uncertainties in K , A , and P_l , respectively. In the following, we assume that δA is negligibly small, although it is recognized that sediment porosity may vary along the beach and across shore (Larson and Kraus, 1994).

The percentage uncertainty in the longshore wave-energy flux factor is

$$\left(\frac{\delta P_l}{P_l} \right) \% = \pm \left(\frac{1}{2} \frac{\delta \gamma}{\gamma} + \frac{5}{2} \frac{\delta H_b}{H_{brms}} + \frac{2\delta \theta_b}{\tan(2\theta_b)} \right) \times 100 \quad (17)$$

where $\delta \gamma$ = uncertainty in the breaker index; and δH_b and $\delta \theta_b$ = uncertainties in H_{brms} and θ_b , respectively. From review of a larger number of data sets comprising more than 400 laboratory measurements, Kaminsky and Kraus (1994) found that γ varied widely, typically between 0.6 and 1.2, with the average equal to the standard value $\gamma = 0.78$. In the following uncertainty analysis, a 10% variation (i.e., $\delta \gamma/\gamma = 0.1$) was applied. In studies measuring waves in deeper water and transforming them to breaking, γ would introduce a much larger uncertainty than given in (17), because it would enter to a higher power. In the present study, the breaker height was directly measured, and the standard $\gamma = 0.78$ was applied.

Eq. (17) was evaluated for the four accepted measurements (Table 3). The largest uncertainty, $\pm 48\%$, in the calculation of the longshore wave-energy flux factor occurred for the smallest waves during Run 2. The large percentage uncertainty associated with Run 6 was caused by the relatively small incident breaking wave angle (Table 2).

The combined uncertainties in the volume-change (rate) measurement [(13)] and in calculation of the longshore wave-energy flux factor [(17)] leads to an uncertainty in K . By equating measured and calculated transport rates, an operation that determines the best-fit K value K_f , and assuming A does not vary, the percentage uncertainty in K_f is given by

$$\frac{\delta K_f}{K_f} = \frac{\delta Q_m}{Q_m} + \frac{\delta P_l}{P_l} \quad (18)$$

where δK_f = uncertainty in K_f . Eq. (18) indicates that the uncertainty δK_f can be large because it is the sum of uncertainties in the volume determination (or other quantity in any measurement procedure) and in the longshore wave-energy flux factor determination. The uncertainties in the measured transport rates and in the wave parameters in the present work are each on the order of 20–50%.

Uncertainties in the empirical coefficient K_f calculated from (18) are given in Table 3. Empirical K -values determined under lower amounts of volume change and longshore wave-energy energy flux (Runs 2 and 6) contain greater uncertainty that the K values obtained under larger longshore energy flux and volume change (Runs 4 and 5). Because instrument and operational error have fixed minimum limits, larger values of measured transport rates and more accurate wave measurements can reduce the uncertainty in K . The K -values obtained from two measurements (Runs 4 and 5) that had a relatively low percentage uncertainty, in both volume and energy flux determinations, agree with K -values obtained from streamer trap measurements (Kraus et al. 1988; Wang et al. 1998a). Large variations in K [e.g., from 0.32 to 1.65 (Dean et al. 1982)] are summarized by Komar (1998) for many previous measurements.

The above analysis based on a Taylor series tends to give a maximum error. For independent random errors, an RMS error approach is possible and would yield a smaller estimate of the uncertainty in the measurements.

CONCLUSIONS

Short-term impoundment at a temporary groin was found to be a promising method for measuring the total longshore sediment transport rate under low-wave energy conditions. The impoundment technique can measure the transport rate for any mixture of sediment type and grain size. The ratio of volumes of updrift accumulation and downdrift erosion serves as an indicator of reliability, providing an objective criterion that incorporates the constancy of the driving forces and the quality of the measurement operation. The reliability indicator for the four accepted measurements in the present study ranged from 0.61 to 1.65. Percentage uncertainty in the transport rate measurement decreased as the magnitude of the volume change increased, because measurement operational error can be considered as approximately fixed.

Maximum sand accumulation was located directly updrift of the groin, whereas maximum erosion was located a certain distance downdrift. The downdrift displacement of maximum erosion is attributed to wave sheltering and passage of a portion of the longshore current through holes in the groin. A similar pattern of shoreline change occurred, except that the point of maximum shoreline advance was located a short distance from, instead of directly at, the groin, as caused by offshore sediment transport along the groin.

The greater volume change obtained downdrift in Run 2 (impermeable groin) suggests that detailed measurement of the current field should be made in future work. It is feasible that the sharp discontinuity in the longshore current at the impermeable groin may have caused acceleration of the current and additional transport than for the water-permeable groins.

For three of the four accepted measurements, the total rate of longshore sediment transport was nearly an order of magnitude less than given by the CERC formula evaluated with the standard empirical coefficient K . The fourth measurement was in approximate agreement with the CERC formula prediction with the standard coefficient value. The range in values of K in these measurements cannot be readily explained by measurement error or uncertainty. Therefore, it is concluded that K is not a constant and that other factors may enter, such

as the breaker type, turbulence intensity, and threshold for sediment transport.

The relatively greater percentage of energy-flux calculation uncertainty was associated with small wave height and small incident wave angle. By increasing the size of the structure and deploying in larger waves, volume change can be increased to reduce uncertainties. In addition, the measurement time interval can be increased to resolve problems of conflicting magnitudes of transport obtained with different measurement methods and with different averaging intervals over a wide range of wave conditions.

It is noted that an error analysis as performed here has not been made for other field measurements comprising the database. It appears worthwhile to estimate bounds for values of the transport rate coefficient K in past measurements and report such values in future measurements to understand the accuracy and limitations of the CERC formula and other empirically based predictive formulas.

ACKNOWLEDGMENTS

Field operations for this study were funded partially by the Florida Department of Environmental Protection and the University of South Florida (USF). The writers thank the USF graduate students for their assistance in the fieldwork. Comments by two anonymous reviewers improved this paper. Ping Wang appreciates the support of Dr. Richard A. Davis at USF and Dr. Gregory W. Stone at Louisiana State University. Review of an early draft of this paper by Julie D. Rosati is appreciated. Nicholas Kraus acknowledges permission granted by the Headquarters, U.S. Army Corps of Engineers, to publish this paper developed under support of the Coastal Inlets Research Program, Inlet Channels and Adjacent Shorelines Work Unit.

APPENDIX I. REFERENCES

- Berek, E. P., and Dean, R. G. (1982). "Field investigation of longshore sediment transport distribution." *Proc., 18th Coast. Engrg. Conf.*, ASCE, Reston, Va., 1620–1639.
- Bodge, K. R. (1987). "Short term impoundment of longshore sediment transport." *Misc. Paper CERC-87-7*, U.S. Army Engineer Waterways Experiment Station, Coastal Engineering Research Center, Vicksburg, Miss.
- Bodge, K. R., and Dean, R. G. (1987). "Short-term impoundment of longshore transport." *Proc., Coast. Sediments '87*, ASCE, Reston, Va., 468–483.
- Bodge, K. R., and Kraus, N. C. (1991). "Critical examination of longshore transport rate magnitude." *Proc., Coast. Sediments '91*, ASCE, Reston, Va., 139–155.
- Bruno, R. O., Dean, R. G., and Gable, C. G. (1980). "Littoral transport evaluations at a detached breakerwater." *Proc., 17th Coast. Engrg. Conf.*, ASCE, Reston, Va., 1453–1475.
- Bruno, R. O., and Gable, C. G. (1976). "Longshore transport at a total littoral barrier." *Proc., 15th Coast. Engrg. Conf.*, ASCE, Reston, Va., 1203–1222.
- Caldwell, J. (1956). "Wave action and sand movement near Anaheim Bay, California." *Tech. Memo. No. 68*, Beach Erosion Board, U.S. Army Engineer Waterways Experiment Station, Vicksburg, Miss.
- Dean, R. G. (1989). "Measuring longshore sediment transport with traps." *Nearshore sediment transport*. R. J. Seymour, ed., Plenum, New York, 313–337.
- Dean, R. G., Berek, E. P., Gable, C. G., and Seymour, R. J. (1982). "Longshore transport determined by an efficient trap." *Proc., 18th Coast. Engrg. Conf.*, ASCE, Reston, Va., 954–968.
- Ebersole, B. A., and Hughes, S. A. (1987). "DUCK85 photopole experiment." *Misc. Paper CERC-87-18*, U.S. Army Engineer Waterways Experiment Station, Coastal Engineering Research Center, Vicksburg, Miss.
- Fairchild, J. C. (1977). "Suspended sediment in the littoral zone at Ventnor, New Jersey, and Nags Head, North Carolina." *Tech. Rep. 77-5*, U.S. Army Engineer Waterways Experiment Station, Coastal Engineering Research Center, Vicksburg, Miss.
- Kaminsky, G., and Kraus, N. C. (1994). "Evaluation of depth-limited breaking wave criteria." *Proc., Oc. Wave Measurement and Analysis*, ASCE, Reston, Va., 180–193.
- Kamphuis, J. W., and Readshaw, J. S. (1978). "A model study of along-shore sediment transport rate." *Proc., 16th Coast. Engrg. Conf.*, ASCE, Reston, Va., 1656–1674.
- Kana, T. W., and Ward, L. G. (1980). "Nearshore suspended sediment

load during storm and post-storm conditions." *Proc., 17th Coast. Engrg. Conf.*, ASCE, Reston, Va., 1158–1173.

Komar, P. D. (1998). *Beach processes and sedimentation*, 2nd Ed., Prentice-Hall, Englewood Cliffs, N.J., 378–424.

Komar, P. D., and Inman, D. L. (1970). "Longshore sand transport on beaches." *J. Geophys. Res.*, 75, 5914–5927.

Kraus, N. C. (1987). "Application of portable traps for obtaining point measurement of sediment transport rates in the surf zone." *J. Coast. Res.*, 2, 139–152.

Kraus, N. C., and Dean, J. L. (1987). "Longshore sediment transport rate distribution measured by trap." *Proc., Coast. Sediment '87*, ASCE, Reston, Va., 818–896.

Kraus, N. C., Gingerich, K. J., and Rosati, J. D. (1988). "Toward an improved empirical formula for longshore sand transport." *Proc., 21st Coast. Engrg. Conf.*, ASCE, Reston, Va., 1183–1196.

Kraus, N. C., and Heilman, D. J. (1998). "Comparison of beach profiles at a seawall and groins, Corpus Christi, Texas." *Shore & Beach*, 66, 4–14.

Kraus, N. C., Isobe, M., Igarashi, H., Sasaki, T. O., and Horikawa, K. (1982). "Field experiments on longshore transport in the surf zone." *Proc., 18th Coast. Engrg. Conf.*, ASCE, Reston, Va., 969–988.

Larson, M., and Kraus, N. C. (1994). "Cross-shore sand transport under random waves at SUPERTANK examined at mesoscale." *Proc., Coast. Dyn. '94*, ASCE, Reston, Va., 204–219.

Mangor, K., Sorenson, T., and Navtoft, E. (1984). "Shore approach at the Danish North Sea coast: Monitoring of sedimentation in a dredge trench." *Proc., 19th Coast. Engrg. Conf.*, ASCE, Reston, Va., 1816–1829.

Moore, G. W., and Cole, J. Y. (1960). "Coastal processes in the vicinity of Cape Thompson, Alaska." *Trace Elements Investigation Rep. No. 753*, U.S. Geological Survey, 41–55.

Ozhan, E. (1982). "Laboratory study of breaker type effect on longshore sand transport." *Mech. of Sediment Transport, Proc., Euromech*, Vol. 156, B. M. Sumer and A. Muller, eds., 265–274.

Rosati, J. D., and Kraus, N. C. (1989). "Development of a portable sand trap for use in the nearshore." *Tech. Rep. CERC-89-11*, U.S. Army Engineer Waterways Experiment Station, Coastal Engineering Research Center, Vicksburg, Miss.

Schoonees, J. S., and Theron, A. K. (1993). "Review of the field data base for longshore sediment transport." *Coast. Engrg.*, 19, 1–25.

Schoonees, J. S., and Theron, A. K. (1994). "Accuracy and applicability of the SPM longshore transport formula." *Proc., 24th Coast. Engrg. Conf.*, ASCE, Reston, Va., 2595–2609.

Shore protection manual (SPM). (1984). U.S. Army Engineer Waterways Experiment Station, Coastal Engineering Research Center, U.S. Government Printing Office, Washington, D.C.

Vitale, P. (1981). "Movable-bed laboratory experiments comparing radiation stress and energy flux factor as predictors of longshore transport rate." *Misc. Rep. No. 81-4*, U.S. Army Engineer Waterways Experiment Station, Coastal Engineering Research Center, Vicksburg, Miss.

Wang, P. (1995). "Surf zone sediment transport on low energy coasts: Field measurement and prediction," PhD dissertation, Dept. of Geol., University of South Florida, Tampa, Fla., 235.

Wang, P. (1998). "Longshore sediment flux in the water column and across the surf zone." *J. Wtrwy., Port, Coast., and Oc. Engrg.*, ASCE, 124(3), 108–118.

Wang, P., Davis, R. A., Jr., and Kraus, N. C. (1998b). "Cross-shore distribution of sediment texture under breaking waves along low-wave energy coasts." *J. Sedimentary Res.*, 68, 497–506.

Wang, P., Kraus, N. C., and Davis, R. A., Jr. (1998a). "Total longshore sediment transport rate in the surf zone: Field measurements and empirical predictions." *J. Coast. Res.*, 14(1), 269–282.

Watts, G. M. (1953). "A study of sand movement at South Lake Worth Inlet, Florida." *Tech. Memo. No. 42*. U.S. Army Engineer Waterways Experiment Station, Beach Erosion Board, Vicksburg, Miss.

APPENDIX II. NOTATION

The following symbols are used in this paper:

A = factor to convert transport rate from mass to volume per unit time;
 g = gravitational acceleration;
 H_{brms} = root-mean-square breaker wave height;
 K = empirical longshore sediment transport coefficient;
 K_f = best-fit K value;
 L_0 = deepwater wavelength;
 M = total number of profiles used in volume calculation;
 m = number of updrift survey lines excluding control line;

n = number of downdrift survey lines excluding control line;
 Post 1 = first beach survey conducted after groin installation;
 Post 2 = second beach survey conducted after groin installation;
 Post 3 = third beach survey conducted after groin installation;
 Pre- = beach survey conducted before groin installation;
 P_l = longshore wave-energy flux factor;
 p = sediment porosity;
 Q_c = calculated total longshore sediment transport rate;
 Q_d = total longshore transport rate calculated from downdrift erosion;
 Q_m = measured longshore sediment transport rate;
 Q_u = total longshore transport rate calculated from updrift accumulation;
 $R_{non-LST}$ = rate of profile-volume change induced by processes other than longshore sediment transport;
 $\tan \beta$ = beach slope;
 $V_{d-total}$ = total volume change induced by longshore transport at downdrift side;
 $V_{u-total}$ = total volume change induced by longshore transport at updrift side;
 v_{c-d} = profile-volume change measured at downdrift control line;
 v_{c-u} = profile-volume change measured at updrift control line;
 v_i = profile-volume change measured at profile i ;
 v_{LST-i} = profile-volume change induced by longshore sediment transport at profile i ;
 $v_{non-LST}$ = profile-volume change induced by processes other than longshore sediment transport;
 Y_s = total cross-shore distance over which volume calculation was made;
 γ = wave breaker index (ratio of wave height to total water depth at breaking);
 Δt = elapsed time between two surveys;
 Δt_c = elapsed time between two surveys on same control line;
 Δt_d = elapsed time from groin installation to survey of mid-point of downdrift grid;
 Δt_{pi} = time interval between completion of groin installation and completion of survey of profile i ;
 Δt_u = elapsed time from groin installation to survey of mid-point of updrift grid;
 ΔV = measured volume change;
 Δx_p = distance between two adjacent survey lines;
 δA = uncertainty in conversion factor A ;
 δH_b = uncertainty in measurement of breaker height;
 δK = uncertainty in K ;
 δK_f = uncertainty in K_f ;
 δP_l = uncertainty in P_l ;
 δQ_c = uncertainty in calculated Q_c ;
 δQ_m = uncertainty in Q_m ;
 δt = uncertainty in Δt ;
 δx_p = uncertainty in Δx_p ;
 δV = uncertainty in total volume change calculation;
 δv = uncertainty in beach profile-volume change calculation;
 δz = uncertainty in elevation measurement;
 $\delta \gamma$ = uncertainty in breaker wave index;
 $\delta \theta_b$ = uncertainty in measurement of incident breaking wave angle;
 θ_b = breaker wave angle;
 ξ_b = surf-similarity parameter defined from breaking wave condition;
 ρ = density of water; and
 ρ_s = density of sediment.

Subscripts

b = wave breaking condition;
 c = calculated quantity;
 i = beach profile number;
 LST = longshore sediment transport;
 l = longshore;
 m = measured quantity; and
 RMS = root mean square.